Science Advances

AAAS

advances.sciencemag.org/cgi/content/full/4/2/eaaq1475/DC1

Supplementary Materials for

Topological transport of sound mediated by spin-redirection geometric phase

Shubo Wang, Guancong Ma, Che Ting Chan

Published 16 February 2018, *Sci. Adv.* **4**, eaaq1475 (2018)
DOI: 10.1126/sciadv.aaq1475

This PDF file includes:

- Mapping between waveguide dispersion and band structure
- fig. S1. Band structures for helical waveguides with different pitches.
- fig. S2. An acoustic interferometer based on spin-redirection geometric phases.
- fig. S3. Full-wave simulations of acoustic interferometers based on spin-redirection geometric phases.

Mapping between waveguide dispersion and band structure

To verify our analytic theory, we perform comparisons between the analytical results and full-wave simulation results for the dispersion relations of the vortex modes in the helical waveguide. In the numerical simulations, the band structure is calculated by using one pitch of the helical waveguide and setting periodic boundary conditions on both ends. The analytical results are given in equation (3) of the main text. For comparisons, we fold the analytical dispersion lines back into the first Brillouin zone. This involves a mapping between the guided wave number k and the Bloch wave number k_B: $k = (D/S)k_B$, which is given by the condition that the waves undergo the same change of phase when propagating through one pitch of the helical waveguide. Here, D is the pitch and S is the total length of the helical waveguide for one pitch. In the limit of $a \ll R, D$, we have $S \approx \sqrt{D^2 + (2\pi R)^2}$. However, for practical parameters used in the experiments and simulations, this relation is only approximately true. Figure S1 shows the comparisons for helical waveguides of different pitch D, where we set a = 3.25 cm and R = 32.5 cm. The circles denote full-wave simulation results while the solid lines are analytical results obtained by direct use of $S = \sqrt{D^2 + (2\pi R)^2}$. Such an approximation lead to deviations between the analytical and numerical results, as in the case of D = 65 cm. As D increases, the analytical results gradually approach the numerical results. The black circles denote the band of the monopole mode, which is not of interest.

To obtain accurate values of S for the cases that do not fulfil the condition $a \ll R, D$, we first determine the centre frequency as $\omega = (\omega_+ + \omega_-)/2$, where $\omega_\pm$ denote the numerical results for the frequency of the $\pm q$ mode. This essentially gives the band structure of the corresponding straight waveguide. By fitting the analytical expression for the dispersion relation of the straight waveguide, i.e., $\omega = c\sqrt{k_r^2 + k^2}$, to this centre frequency band structure, we obtain the correct values of *S*, which can be used for the mapping of $k = (D/S)k_{\mathrm{B}}$. The results in Fig. 2b of the main text are obtained in this way.

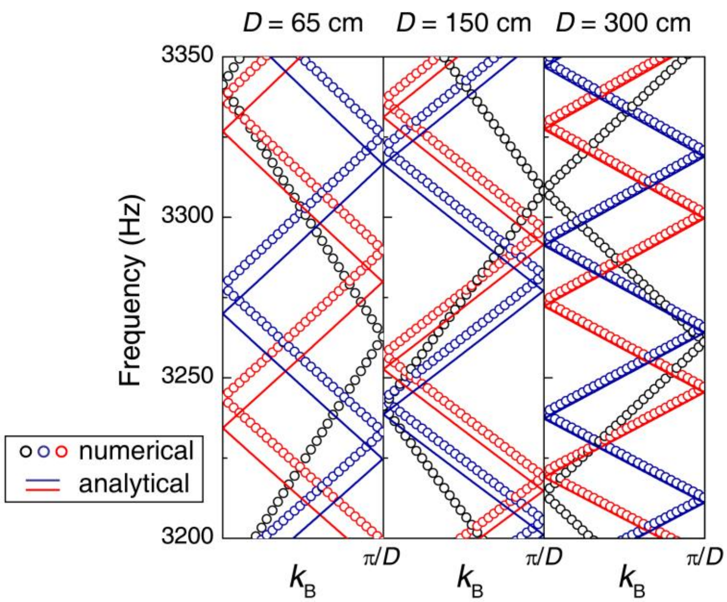

fig. S1. Band structures for helical waveguides with different pitches. The circles denote the full-wave simulation results while the solid lines denote the analytical results, which are obtained by folding the band dispersion of equation (3) into the first Brillouin zone using the mapping of $k = (D/S)k_{\mathrm{B}}$. Here, we make approximations and set $S = \sqrt{D^2 + (2\pi R)^2}$.

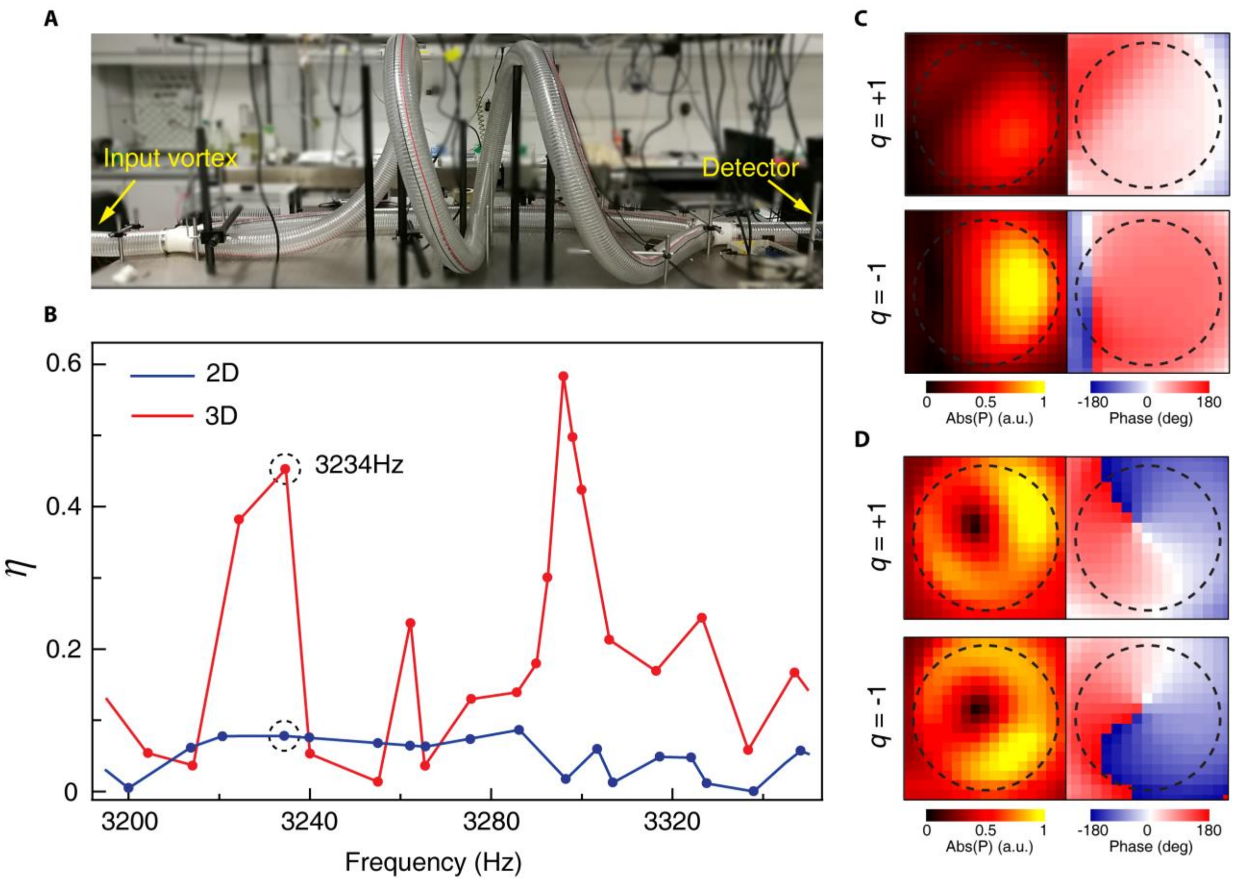

fig. S2. An acoustic interferometer based on spin-redirection geometric phases. (**A**) A 3D acoustic interferometer consisting of a helical waveguide and a bent waveguide. (**B**) The transmission contrast η (see main text for definition) of the $q = \pm 1$ vortices as a function of frequency for the 2D (not shown) and 3D interferometers. The 2D setup is obtained by unwinding the helical waveguide so that the two waveguide branches lie on a 2D plane. (**C**) The normalized magnitude and the phase of the output pressure field of the $q = \pm 1$ vortices at the frequency f = 3,234 Hz for the 3D case. (**D**) The normalized magnitude and phase of the output pressure field of the $q = \pm 1$ vortices at the frequency f = 3,234 Hz for the 2D case, which has mirror symmetry.

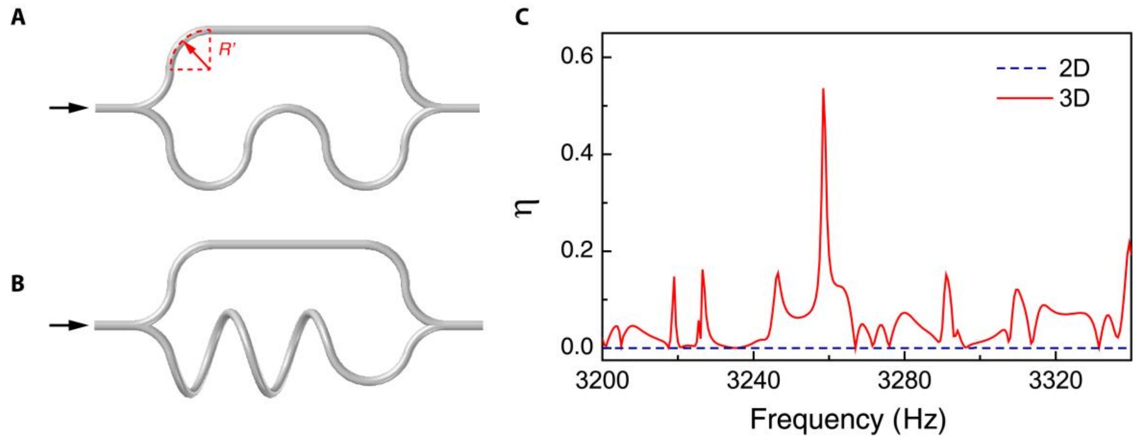

fig. S3. Full-wave simulations of acoustic interferometers based on spin-redirection geometric phases. The configurations of the 2D and 3D interferometers are shown in (**A**) and (**B**), respectively, where the $q = \pm 1$ vortices are excited at the left end. The arc parts of the waveguide in both (A) and (B) have radii of *R'* = 34 mm. The helical part has radius *R* and pitch *D* with the same values as in the experiments. (**C**) The simulation results of the transmission contrast η for the 2D and 3D interferometers.